Acta Materialia 125 (2017) 187–195

Contents lists available at ScienceDirect

Acta Materialia

journal homepage: www.elsevier.com/locate/actamat

Full length article

Dilatancy in semi-solid steels at high solid fraction

K.M. Kareh [a], C. O'Sullivan [b], T. Nagira [c], H. Yasuda [d], C.M. Gourlay [a, *]

[a] Department of Materials, Imperial College London, Prince Consort Road, London, UK
[b] Department of Civil Engineering, Imperial College London, Prince Consort Road, London, UK
[c] Department of Adaptive Machine Systems, Osaka University, Suita, Osaka, Japan
[d] Department of Materials Science and Engineering, Kyoto University, Sakyo Ku, Kyoto, Japan

ARTICLE INFO

Article history:
Received 6 July 2016
Received in revised form
25 November 2016
Accepted 29 November 2016

Keywords:
Semi-solid
In situ
Carbon steel
Porosity

ABSTRACT

The study of mushy-zone deformation in steels is important for limiting defect formation in continuous casting. Here, we use *in situ* synchrotron radiography to quantify the shear deformation mechanisms of an equiaxed carbon steel at a solid fraction >0.9 and to understand how these mechanisms lead to casting defects. We show that the grain assembly undergoes shear-induced dilation (Reynolds' dilatancy) which opens liquid-filled fissures and cracks at high solid fraction. We further show a complex interaction between grain rearrangement, grain deformation and local coarsening, where rearrangement reduces the grain-grain contact area and coordination number which alters the stress network and also drives coarsening as grains move apart.

1. Introduction

Deformation of the solidifying shell is an important part of the continuous casting of steel [1,2]. For example, unwanted deformation caused by bulging or roll misalignment leads to macrosegregation [3–5] and can cause internal cracking [1]. On the other hand, external deformation can be beneficial such as the application of a 'soft reduction', a small rolling reduction (e.g. a few % strain) near to the end of the sump to compensate for solidification shrinkage and reduce centreline segregation and porosity [6–8]. Despite this importance, there remains only limited understanding of the mechanical behavior of the mushy-zone in steels and, in particular, of their microstructural response to load and how this leads to defects. This is an obstacle to the development of thermo-mechanical models and, therefore, to defect mitigation strategies and the design of improved processes.

During continuous casting, the semi-solid region spans the full range of solid fraction from the edge of the fully-solid shell, through a mushy region to the liquid interior and, therefore, external loads act on a complex solid fraction gradient with a microstructure that can be columnar, equiaxed or mixed. It is known that the most severe deformation defects occur in high solid fraction material [1,9], where liquid flow is difficult due to the low permeability; this can result in pore opening or semi-solid cracking, and the motion of liquid gives rise to more severe macrosegregation because C_L-C_0 is larger at higher solid fraction. High solid fraction deformation has also been identified as one of the least understood areas of continuous casting [10].

In this paper, we aim to investigate the deformation mechanisms operating in equiaxed semi-solid steels undergoing shear loading at high solid fraction, which is relevant to regions within the continuous caster being deformed during the final stages of solidification. We study an equiaxed microstructure since this is a desired continuous casting microstructure that can be achieved industrially by, for example, electromagnetic stirring [11]. In order to directly image the microstructural response to load, we use synchrotron radiography building on the techniques developed for steel solidification by Yasuda et al. [12]. We study deformation under conditions of fully-fed deformation and deformation with inadequate feeding with the following specific aims: (i) to identify and quantify the deformation mechanisms, (ii) to compare the observed mechanisms with those assumed in models of the continuous casting process and those measured in steels at lower solid fraction previously [13–15], and (iii) to develop an

* Corresponding author.
E-mail address: c.gourlay@imperial.ac.uk (C.M. Gourlay).

http://dx.doi.org/10.1016/j.actamat.2016.11.066
1359-6454/

understanding of how shear deformation can generate macro-segregation and cracking during the final stages of solidification.

2. Experimental

A sample of Fe-0.1C-0.6Mn-0.3Si-0.3P (mass pct) was cut with dimensions of 10 × 10 mm with a thickness of approximately 180 μm. The synchrotron experimental procedure has been described in previous publications [8,14,16] and is schematized in Fig. 1. It consisted of the specimen being held in a square, hollowed out, 200 μm thick Al_2O_3 mould sandwiched in between two 100 μm thick sapphire plates and held in between two boron nitride plates. A 150 μm Al_2O_3 pushplate was then inserted at the bottom of the specimen to push half the specimen up and produce direct shear loading at a constant pushplate speed of 10 μm s^{-1}, which corresponds to a global strain rate of 0.001 s^{-1}. Radiographic images were captured on a CCD camera at the BL20B2 beamline at the SPring-8 synchrotron in Hyogo, Japan, with a beam energy of 22 keV and an exposure time of 500 ms. The working field of view was 4.8 × 4.8 mm with a pixel size of 4.7 μm.

X-ray images were processed using commercial softwares ImageJ [17], Avizo 7.0.1 [18] (Visualization Science Group, Mérignac, France) and MATLAB 7.1 [19] (The Mathworks Inc., MA, USA). Images were cropped and aligned using a normalised mutual information metric similarity measure [20]. Due to radiography artefacts, the solid phase was manually thresholded and the grains manually separated. Grains were tracked using code from Refs. [21,22] and translation calculated from the tracked coordinates of the centroid of each grain. Rotation and major length were calculated using principal component analysis [23,24]. By examining the change in the width of the liquid channels between the grains with the motion of the pushplate, grain neighbors were determined via a 3 × 3 pixel morphological dilation of each grain and its intersection with neighboring grains. Grains were deemed not to touch if the greyscale profile between their centroids showed greyscale values higher than 10,600 over 5 pixels. Examples of such boundaries are shown in Figs. S1 and S2 of the Supplementary Information. Determining grain neighbors allowed the calculation of the coordination number (i.e. the number of contacting neighbors of each grain), as well as the contact index, which is defined as the fraction of perimeter pixels that are contact pixels (i.e. grain-grain contacts). A contact pixel was defined here as any pixel belonging to both a grain and one of its neighbors after the morphological dilation operation and satisfying the greyscale intensity requirement, and it would cease being a contact pixel once the grains stop overlapping after morphological dilation.

3. Results and discussion

3.1. Shear-induced dilation

The initial undeformed microstructure is shown in Fig. 2(a). The solid grains appear dark grey and quasi-polygonal, and are separated by thin liquid channels that appear light grey (Fig. 2(a)). The dark features are due to diffraction of the γ-Fe crystals or of the sapphire confining sheets (the dark bands). The bright white feature to the bottom-left of the field of view is a pre-existing pore.

The projected area fraction of liquid is ~1% as estimated by the thin liquid channels in between the grains, but the volume fraction of liquid is higher as there is some additional liquid in front of and behind the solid in the X-ray direction of the thin sample. There is also some liquid entrapped within the grains which appears in the radiography images as 'mottling' in each grain (e.g. Fig. 3). This greyscale mottling within grains remained constant throughout the experiment and the shape of the internal liquid spaces did not measurably change, indicating that the entrapped liquid remains confined within each grain. Similar entrapped liquid is commonly created by semi-solid processing routes (such as forced convection or extended semi-solid coarsening) [25,26], and is usually treated as effective solid in semi-solid rheology. Thus, the effective solid fraction in the field of view can be conservatively stated as >0.9.

Four stages of deformation are shown in Fig. 2, spanning ~900 μm of pushplate displacement, to give an overview of the range of phenomena that occur during high solid fraction shear deformation. Note that the pushplate moves vertically upwards from the bottom right of each image. It can be seen that, as the pushplate intrudes into the sample, the space between the grains increases and fills with liquid, seen in lighter grey in Fig. 2(b). At the same time, the pore to the left-side of the field of view opens (cf. Fig. 2(a) *vs.* (b)). With increasing pushplate displacement (Fig. 2(c) and (d)), further pores and cracks (bright regions) develop throughout the sample.

The opening of spaces between the grains as the pushplate shears the sample is the phenomenon of shear-induced dilation or Reynold's dilatancy [27] which is widespread in particulate materials [28–30] and has been shown to occur in semi-solid alloys [13,31,32]. This is shown at higher magnification in Fig. 3 and supplementary movie S3, both showing region (m) highlighted in Fig. 2(a). It is clear, particularly in the supplementary movie S3, that the grains push and lever each other apart as they rearrange under

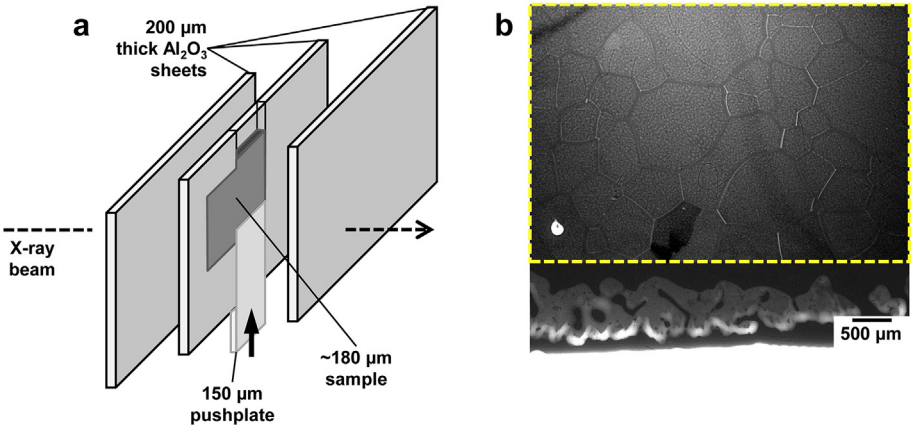

Fig. 1. Schematic of the experimental setup. a) Exploded view of the radiography setup and b) radiograph of the carbon steel sample before deformation, with the region of interest that will be analysed outlined in yellow. (For interpretation of the references to colour in this figure legend, the reader is referred to the web version of this article.)